NUMERICAL ANALYSIS ON THRUST CHARACTERISTICS OF A CYCLOROTOR: EFFECT OF NUMBER OF BLADES

Manabu Saito
Department of Mechanical Engineering and Science
Kyoto University
Kyoto daigaku-Katsura, Nishikyo-ku, Kyoto 615-8540, Japan
saito.manabu.63z@st.kyoto-u.ac.jp

Jun Nagao
Department of Mechanical Engineering and Science
Kyoto University
Kyoto daigaku-Katsura, Nishikyo-ku, Kyoto 615-8540, Japan
nagao.jun.87c@st.kyoto-u.ac.jp

Ryoichi Kurose
Department of Mechanical Engineering and Science
Kyoto University
Kyoto daigaku-Katsura, Nishikyo-ku, Kyoto 615-8540, Japan
kurose@mech.kyoto-u.ac.jp

ABSTRACT

A cyclorotor generally consists of three to six blades, and depending on the instantaneous position of the blades, the total thrust produced by the blades oscillates inevitably and prompts the fuselage to vibrate. In this study, the thrust characteristics of a cyclorotor among different numbers of blades are numerically investigated to explore the optimal configurations of a cyclorotor for better aerodynamic performance, such as suppressing the thrust oscillations. The results show that out of three- to six-bladed cyclorotors, the four-bladed cyclorotor features the largest thrust oscillation magnitude. The thrust generation characteristics can be explained by considering the thrust generation of each blade at each azimuthal angle and the relative position of the blades, and the four-bladed cyclorotor was found that the thrust generation of two blades located on the opposite side synchronize.

INTRODUCTION

A cyclorotor is a propulsion system that rotates multiple blades around an axis, which is in parallel to the blades' spanwise direction, and while doing so, the scheduled angle of attack of the blades relative to the tangential direction of the rotating circle enables the blades to generates thrust. By changing the schedule of the angle of attack of the blades, it can generate thrust in any direction and magnitude instantaneously. This results in excellent maneuverability in the air without changing the orientation of the cyclorotor. Also, the noise generated from a cyclorotor is expected to be smaller compared with the conventional propellers as a cyclorotor operates at lower rotational speeds compared with conventional propellers. This feature of less noise generation makes a cyclorotor a suitable propulsion system for Urban Air Mobility (UAM). However, as the development of the cyclorotor is still in the experimental stage (Benedict *et al.* (2010); Sirohi *et al.* (2007)), improvements in aerodynamic performance are required for practical applications. For example, Moble (2010) experimentally investigated the effects of rotational speed, blade pitch control, blade shape, and the number of blades on the aerodynamic performance of a cyclorotor. The results showed decreasing thrust generation efficiency for each blade as the number of blades increased.

However, the detailed aerodynamical understanding behind this decrease in thrust generation efficiency has not been fully investigated due to the complexity of experimental apparatus and flow fields generated by a cyclorotor. To further investigate the flow field in detail, several numerical studies were conducted using Reynolds-averaged Navier Stokes (RANS) solver (Halder & Benedict (2022); Hu *et al.* (2016)) and large-eddy simulations (LES) (Saito *et al.* (2024)), but the effect of the number of blades to the aerodynamic performance of the cyclorotor considering the intense interaction between the blades and the downwash is not fully investigated.

Therefore, in this study, several LES of cyclorotors for different numbers of blades are conducted to investigate the thrust generation characteristics of cyclorotors among different numbers of blades and explore the optimal configurations of a cyclorotor.

NUMERICAL PROCEDURE

In this study, several LES are conducted to investigate the effect of the number of blades on the thrust generated by cyclorotors. The geometrical configuration of the cyclorotor follows the experiment of a six-bladed cyclorotor conducted by Sirohi *et al.* (2007) whose parameters are listed in Table 1.

Table 1: Coefficients of thrust, C_T, and power, C_P.

Blade shape	NACA0010
Blade chord [mm]	25.4
Blade span [mm]	150
Number of blades	3, 4, 5, 6
Rotational speed [rev/min]	800
Rotational radius [mm]	60

The governing equations are the following conservation equations of mass and momentum for the incompressible fluid.

$$\nabla \cdot (\tilde{u}) = 0, \tag{1}$$

$$\bar{\rho}\frac{\partial \tilde{u}}{\partial t} + \bar{\rho}\nabla \cdot (\tilde{u}\tilde{u}) = -\nabla \bar{p} + \nabla \cdot \tilde{\tau} + f, \tag{2}$$

where ρ is the density, u is the velocity, p is the pressure, τ is the viscous stress tensor, and f is the imaginary external force imposed using the diffuse-interface immersed boundary method Peskin (2002). In the above equations, the overbar $\bar{}$ indicates spatial filtering of a physical quantity, and the tilde $\tilde{}$ indicates Favre filtering. The unresolved subgrid-scale modelling is conducted using the Dynamic Smagorinsky model Lilly (1992); Moin *et al.* (1991).

The computational domain is 40R, 40R, and 20R in x-, y-, and z-directions, respectively, where R is the rotational radius. The origin is set at the rotational axis of the cyclorotor in x- and y- direction, and mid-span in z-direction. Outflow boundary conditions are set in x- and y-directions. Symmetric boundary condition is set in negative z-direction at z = 0 mm, and outflow boundary condition is set in positive z-direction. Initial conditions are static air at 1 atm and 300 K, and the thrust is generated in positive y-direction. The minimum grid sizes are 200 µm in x-, y- and z-directions, and the number of grid points in each direction, nx, ny, and nz are 900, 940, and 255, respectively. The LES are performed using an in-house solver referred to as FK^3 (Kurose (n.d.)), which consists of a fractional-step method that employs a pressure-based semi-implicit algorithm for incompressible flows. The spatial derivatives of the convective terms in the momentum equation are approximated using Kawamura-Kuwahara scheme (Kawamura & Kuwahara (1984)).

RESULTS AND DISCUSSION

The LES are validated in a previous study (Saito & Kurose (to be submitted)) by comparing the thrust and power coefficient, C_T and C_P, of the six-blade cyclorotor with that of the experiment (Sirohi et al., 2007), and shows an acceptable agreement as shown in Table 2.

$$C_T = \frac{T}{\rho(\pi b_r d)(\omega R)^2} \tag{3}$$

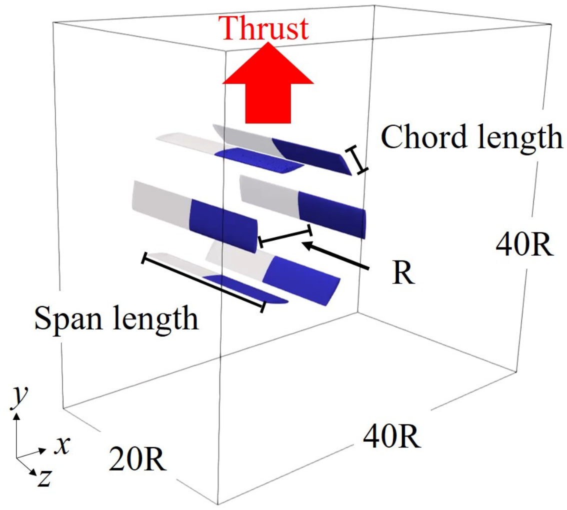

Figure 1: Computational domain for the cyclorotor consisting of six blades (Saito & Kurose (to be submitted)). Blue region on the blades denotes the region where the present LES analyzes.

$$C_P = \frac{P}{\rho(\pi b_r d)(\omega R)^3} \tag{4}$$

Table 2: Coefficients of thrust, C_T, and power, C_P.

[-]	LES	Experiment
C_T	0.04661	0.04573
C_P	0.02681	0.02941

Here, T [N], P [W], b_r [m], d [m], and ω [1/s] are the thrust, the power, the spanwise length, the rotational diameter and the rotational speed of the blades, respectively.

To observe the differences in the generated flow field among different numbers of blades, Fig. 2 shows the comparison of the three-dimensional generated flow field by the three to six-bladed cyclorotors by visualizing the isosurface of the secondary invariant, Q, of 300,000 colored by the velocity in y-direction. It can be observed that as the number of blades increases, the turbulence generation in the cyclorotor increases. The effect of this generated flow field on the aerodynamic performance of the cyclorotors is discussed later.

To qualitatively investigate the thrust generation characteristics among different numbers of blades, Fig. 3 shows the comparison of the statistical thrust coefficient variations among cyclorotors consisting of three to six blades. The lines at the center of the boxes indicate the time-averaged thrust generation. The top and bottom lines of the grey boxes indicate the first and third quartiles of the instantaneous thrust generation of cyclorotors, which are used to evaluate the amplitude of the thrust oscillation. It is apparent that the time-averaged thrust generation of each cyclorotor increases as the number of blades increases, as it was discussed in previous studies (Benedict *et al.* (2010, 2011)). Also, the increase in thrust generation is not proportional to the increase in the number of blades.

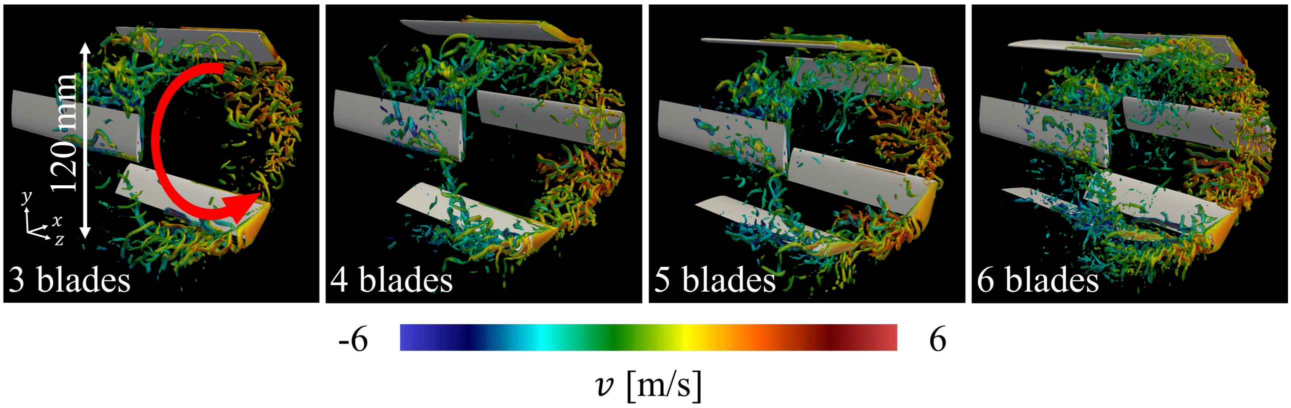

Figure 2: Comparison of 3D visualization of the flow among cyclorotors consisting of three to six blades (isosurfaces of q-criterion at 300,000 [$1/s^2$] and contours of velocity in y-direction).

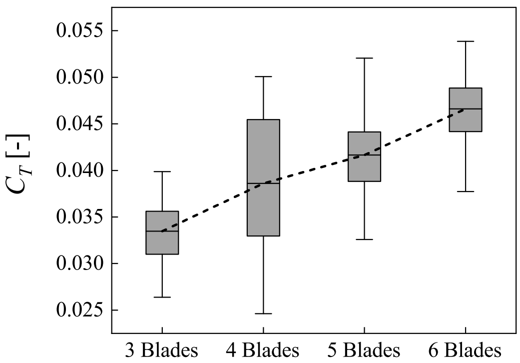

Figure 3: Comparison of the statistical thrust variations among cyclorotors consisting of three to six blades.

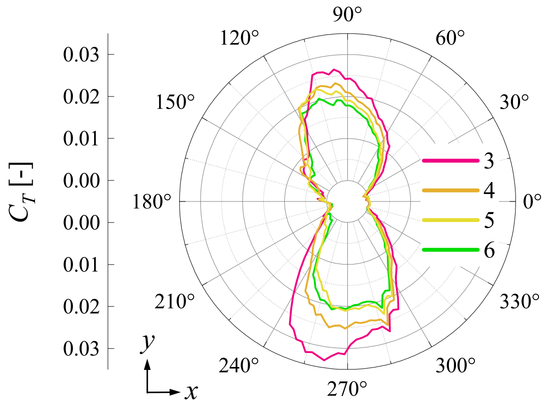

Figure 4: Comparison of thrust coefficients corresponding to the azimuthal angle between cyclorotors consisting of three to six blades.

This is due to the decreased efficiency of the thrust generation of each blade.

To evaluate the decreased efficiency of the blades, Fig. 4 shows the comparison of thrust coefficients corresponding to the azimuthal angle between cyclorotors consisting of three to six blades. As the number of blades increases, the thrust coefficients for most of the azimuthal angle decrease. The decrease in the thrust generation is significant around the azimuthal angle of 260°. Because of this decrease in each blade's thrust efficiency, the increase in the thrust generation is not proportional to the increase in the number of blades, but slightly smaller.

Also, in Fig. 3, among three- to six-bladed cyclorotors, the amplitude of the thrust oscillation of the four-bladed cyclorotor is the largest and more than twice as large as the rest of the cases. To investigate the reason behind this, the time variation of thrust coefficient, C_T, of each blade and total of the coefficient is compared among four- and five-bladed cyclorotors in Fig. 5. In the four-bladed cyclorotor, the thrust generation of every two blades synchronizes, whereas in the five-bladed cyclorotor, the thrust generation is distributed in time. This can be anticipated by considering the geometrical position of the blades and the thrust coefficients corresponding to the azimuthal angle. In Fig. 4, the blade's thrust in all numbers of blades peaks almost every 180°.

On the other hand, the blades in the three- to six-bladed cyclorotors are located every 120°, 90°, 72°, and 60°, respectively. Therefore, out of all cyclorotors, only in the four- and six-bladed cyclorotors do two blades generate large thrust at the same time, causing thrust generation synchronization. Furthermore, in the four- and six-bladed cyclorotors, this synchronization occurs every 90°- and 60°- rotations, respectively. As the thrust generation efficiency of the blade is larger in the four-bladed cyclorotor, the thrust generation synchronization causes a larger oscillation amplitude than in the six-bladed cyclorotor. As a result, the total thrust generation of the four-bladed cyclorotor features the largest amplitude in thrust oscillation out of the three- to six-bladed cyclorotors. When designing the number of blades in a cyclorotor, in terms of aerodynamic aspect, avoiding the synchronization of the thrust generation of each blade is effective in reducing the vibration of the cyclorotor.

In addition, the cause of the decrease in thrust efficiency as the number of blades increases is investigated. Figure 6 shows the comparison of time-averaged velocity in y-direction between cyclorotors consisting of three to six blades at (x,y) = (0 mm, 30 mm), which is below the blades on the suction side of the cyclorotor. It can be seen that the magnitude of the downwash velocity increases as the number of blades increases. This induces a decrease in the effective angle of attack on the blades around the azimuthal angle of 270°, which de-

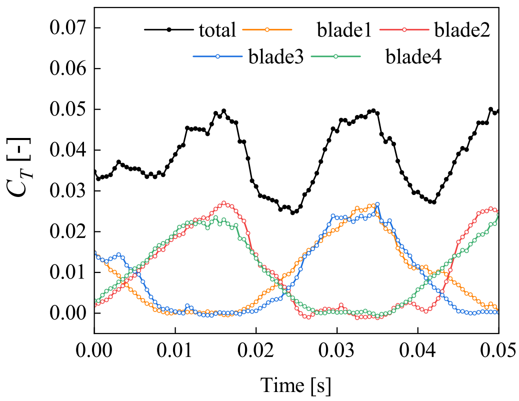

a 4-bladed cyclorotor

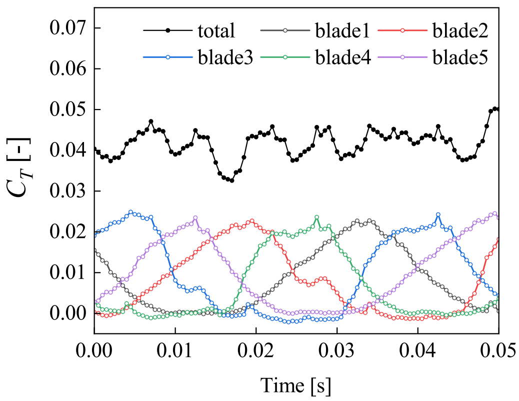

b 5-bladed cyclorotor

Figure 5: Comparison of instantaneous thrust distribution between 4- and 5-bladed cyclorotors.

creases the thrust generation.

CONCLUSIONS

Several LES of cyclorotors for different numbers of blades were performed to investigate the thrust generation characteristics of a cyclorotor among different numbers of blades and explore the optimal configurations of a cyclorotor. The results showed an increase in the thrust generation magnitude as the number of blades in a cyclorotor increased, but the thrust generation of each blade decreased, as discussed by Moble (2010). This was due to the increase in the downwash velocity as the number of blades increased, which resulted in a decrease in the effective angle of attack of each blade, hence less thrust generation. In addition, out of the three- to six-bladed cyclorotors, the four-bladed cyclorotor featured the largest thrust oscillation due to the synchronization of the thrust generation of the opposite blades.

REFERENCES

Benedict, Moble, Jarugumilli, Tejaswi & Chopra, Inderjit 2011 Experimental optimization of mav-scale cycloidal rotor performance. *Journal of the American Helicopter Society* **56** (2), 22005–22005.

Benedict, Moble, Ramasamy, Manikandan & Chopra, Inder-

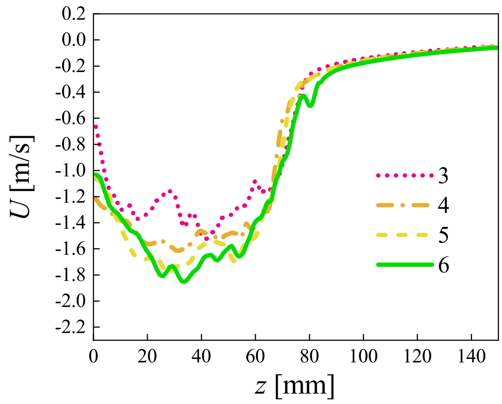

Figure 6: Comparison of time-averaged velocity in y-direction between cyclorotors consisting of three to six blades from z = 0 mm to z = 150 mm at (x, y) = (0 mm, 30 mm).

jit 2010 Improving the aerodynamic performance of micro-air-vehicle-scale cycloidal rotor: an experimental approach. *Journal of Aircraft* **47** (4), 1117–1125.

Halder, Atanu & Benedict, Moble 2022 Understanding upward scalability of cycloidal rotors for large-scale uas applications. *Journal of the American Helicopter Society* **67** (4), 1–15.

Hu, Y, Du, F & Zhang, HL 2016 Investigation of unsteady aerodynamics effects in cycloidal rotor using rans solver. *The Aeronautical Journal* **120** (1228), 956–970.

Kawamura, Tetuya & Kuwahara, Kunio 1984 Computation of high reynolds number flow around a circular cylinder with surface roughness. In *22nd Aerospace Sciences Meeting*, p. 340.

Kurose, Ryoichi n.d. About in-house code FK^3. http://www.tse.me.kyoto-u.ac.jp/members/kurose/link.php, (visited on 4/12/24).

Lilly, Douglas K 1992 A proposed modification of the germano subgrid-scale closure method. *Physics of Fluids A: Fluid Dynamics* **4** (3), 633–635.

Moble, Benedict 2010 *Fundamental understanding of the cycloidal-rotor concept for micro air vehicle applications*. University of Maryland, College Park.

Moin, Parviz, Squires, Kyle, Cabot, W & Lee, Sangsan 1991 A dynamic subgrid-scale model for compressible turbulence and scalar transport. *Physics of Fluids A: Fluid Dynamics* **3** (11), 2746–2757.

Peskin, Charles S 2002 The immersed boundary method. *Acta numerica* **11**, 479–517.

Saito, Manabu & Kurose, Ryoichi to be submitted Numerical investigation on blade-tip vortex effect in a cyclorotor system .

Saito, Manabu, Nagao, Jun, Yamada, Takuto, Pillai, Abhishek Lakshman & Kurose, Ryoichi 2024 Large-eddy simulation of blade-turbulence interaction in a cyclorotor system. *Aerospace Science and Technology* **146**, 108921.

Sirohi, Jayant, Parsons, Eric & Chopra, Inderjit 2007 Hover performance of a cycloidal rotor for a micro air vehicle. *Journal of the American Helicopter Society* **52** (3), 263–279.